

Mohammad Abolhassani, Adeline Guais, Philippe Chaumet-Riffaud, Annie J. Saso and Laurent Schwartz

Am J Physiol Lung Cell Mol Physiol 296:657-665, 2009. First published Jan 9, 2009;
doi:10.1152/ajplung.90460.2008

You might find this additional information useful...

This article cites 36 articles, 14 of which you can access free at:

<http://ajplung.physiology.org/cgi/content/full/296/4/L657#BIBL>

Updated information and services including high-resolution figures, can be found at:

<http://ajplung.physiology.org/cgi/content/full/296/4/L657>

Additional material and information about *AJP - Lung Cellular and Molecular Physiology* can be found at:

<http://www.the-aps.org/publications/ajplung>

This information is current as of March 25, 2009 .

Carbon dioxide inhalation causes pulmonary inflammation

Mohammad Abolhassani,¹ Adeline Guais,² Philippe Chaumet-Riffaud,^{3,4} Annie J. Sasco,⁵ and Laurent Schwartz⁶

¹BCG Department, Pasteur Institute of Iran, Tehran, Iran; and ²Biorébus, Paris; ³Université Paris-Sud, EA4046, UFR de Bicêtre, Le Kremlin-Bicêtre; ⁴AP-HP, CHU de Bicêtre, Service de Biophysique et de Médecine Nucléaire, France; ⁵Epidemiology for Cancer Prevention, INSERM U897, ISPED, Victor Segalen Bordeaux 2 University, Bordeaux, France; and ⁶Service de Radiothérapie, Hôpital Pitié-Salpêtrière, Paris, France

Submitted 27 August 2008; accepted in final form 8 January 2009

Abolhassani M, Guais A, Chaumet-Riffaud P, Sasco AJ, Schwartz L. Carbon dioxide inhalation causes pulmonary inflammation. *Am J Physiol Lung Cell Mol Physiol* 296: L657–L665, 2009. First published January 9, 2009; doi:10.1152/ajplung.90460.2008.—The aim of this study was to assess whether one of the most common poisons of cellular respiration, i.e., carbon dioxide, is proinflammatory. CO₂ is naturally present in the atmosphere at the level of 0.038% and involved in numerous cellular biochemical reactions. We analyzed in vitro the inflammation response induced by exposure to CO₂ for 48 h (0–20% with a constant O₂ concentration of 21%). In vivo mice were submitted to increasing concentrations of CO₂ (0, 5, 10, and 15% with a constant O₂ concentration of 21%) for 1 h. The exposure to concentrations above 5% of CO₂ resulted in the increased transcription (RNase protection assay) and secretion (ELISA) of proinflammatory cytokines [macrophage inflammatory protein-1 α (MIP-1 α), MIP-1 β , MIP-2, IL-8, IL-6, monocyte chemoattractant protein-1, and regulated upon activation, normal T cell expressed, and, presumably, secreted (RANTES)] by epithelial cell lines HT-29 or A549 and primary pulmonary cells retrieved from the exposed mice. Lung inflammation was also demonstrated in vivo by mucin 5AC-enhanced production and airway hyperreactivity induction. This response was mostly mediated by the nuclear translocation of p65 NF- κ B, itself a consequence of protein phosphatase 2A (PP2A) activation. Short inhibiting RNAs (siRNAs) targeted toward PP2Ac reversed the effect of carbon dioxide, i.e., disrupted the NF- κ B activation and the proinflammatory cytokine secretion. In conclusion, this study strongly suggests that exposure to carbon dioxide may be more toxic than previously thought. This may be relevant for carcinogenic effects of combustion products.

tobacco smoke; protein phosphatase 2A; nuclear factor- κ B

CARBON DIOXIDE (CO₂) is naturally present in the atmosphere where its concentration is ~0.038% (0.29 mmHg or 380 ppm). It is a colorless gas that is heavier than air and which has a faintly pungent odor.

Carbon dioxide is a normal constituent of the body arising from cellular respiration. It diffuses from the tissues into the surrounding capillaries and is carried by blood in chemical combination with hemoglobin, in physical solution as dissolved carbon dioxide, carbonic acid, or bicarbonate ions, and as minor amounts of other carbamino compounds (carbon dioxide in combination with plasma proteins). The partial pressure of carbon dioxide in pulmonary capillary blood is ~7% or 46 mmHg, which is greater than that in alveolar air (6% or 40 mmHg). The gas is exchanged freely through the alveolar membrane by diffusion, because of the concentration

gradient existing between the blood and the air in the alveoli, and is thus released from the lungs by convection.

Carbon dioxide is not an inert molecule. It reacts with water to undergo hydration and release carbonic acid (CO₂ + H₂O \leftrightarrow H₂CO₃ \leftrightarrow H⁺ + HCO₃⁻). As for other buffers, pH is related to concentrations of CO₂ and bicarbonates according to the Henderson-Hasselbalch equation. There are several reports in the literature suggesting that exposure to high concentrations of CO₂ can be deleterious. These, mostly old, studies were essentially conducted to assess the effects of breathing in a confined environment such as a submarine or space ship (25, 28).

There are little, if any, data on the toxicity of carbon dioxide released during combustion. Analysis of primary tobacco smoke demonstrates the presence of a very high concentration of 12.5% carbon dioxide (7, 26). Similar concentrations are detected in fuel gas (~8.8%) or coal power plant emissions (~13.7%) (4).

Several studies assessed the acute effects of smoking on mouse models, and all demonstrated the development of inflammation and oxidative stress (35). For instance, 1 h after cigarette smoke exposure, alveolar macrophages from bronchoalveolar lavage showed an increase NF- κ B activity, the release of inflammatory mediators IL-1 β and monocyte chemoattractant protein-1 (MCP-1), and cellular infiltration of activated macrophages in lung tissue (5). Furthermore, acute smoke exposure can result in tissue damage (increased lipid peroxidation and extracellular matrix degradation) 6 h after the inhalation of the smoke of two cigarettes (6).

In this work, we performed a feasibility study to confirm the inflammatory effect of carbon dioxide, decipher its mechanism of action, and suggest that the toxicity of smoke may be, at least partially, mediated by carbon dioxide.

MATERIALS AND METHODS

Animals. BALB/c mice were obtained from the Centre d'Élevage R. Janvier (Le Genest Saint Isle, France) and maintained in accordance with the European Community's guidelines concerning the care and use of laboratory animals. All aspects of the protocol conformed with the requirements of the laboratory's approval for animal research (1987 regulation) and were approved by a research ethic board.

Cell cultures. The human colon and pulmonary cancer cell lines, HT-29 and A549 [cat. nos. HTB-38 and CCL-185; American Type Culture Collection (ATCC)] were cultured in DMEM (Gibco) supplemented with 10% decomplemented FBS (Eurobio, Les Ulis,

Address for reprint requests and other correspondence: L. Schwartz, Service de Radiothérapie Hôpital Pitié-Salpêtrière, bd. de l'Hôpital, 75013 Paris, France (e-mail: laurent.schwartz@polytechnique.edu).

The costs of publication of this article were defrayed in part by the payment of page charges. The article must therefore be hereby marked "advertisement" in accordance with 18 U.S.C. Section 1734 solely to indicate this fact.

France) and 1% nonessential amino acids in a humid atmosphere with various concentrations of CO₂ at 37°C for up to 48 h with a constant O₂ concentration of 21%. During these incubations, pH of the culture medium was measured every 6 h with a pH meter (PHM210 MeterLab; Radiometer Analyticals).

ELISA. Cytokine secretions into the supernatants of HT-29 and A549 human cells (cultivated in 25-cm² flask) were quantified after a 48-h culture using the DuoSet ELISA development kit (R&D Systems, Minneapolis, MN) for human IL-8, IL-6, and MCP-1, as already described (2).

In an independent experiment, HT-29 cells were cultivated in six-well plates, and the pH of the culture medium was modified by addition of HCl (0.8 N) to obtain pH 6.5, 6.7, and 6.9 compared with control (pH 7.28). IL-8 and IL-6 proinflammatory cytokine secretions in the supernatants were measured every 6 or 12 h for up to 48 h. Similarly, macrophage inflammatory protein-2 (MIP-2) secretion by mouse pulmonary cells was measured in the supernatants after 20 h of culture.

RNase protection assays. RNA was extracted from HT-29 or mouse pulmonary cells using RNeasy kit (Qiagen). The mRNA expression was measured by the RiboQuant multiprobe RNase protection assay (BD Biosciences Pharmingen, San Diego, CA). Template RNA probes were transcribed using the cDNA template sets hCK-5 for human or mCK-5C for mouse extracts according to the manufacturer's instructions. For transcription, except for Biotin-16-UTP (Roche Diagnostics, Mannheim, Germany), all reagents were supplied by the manufacturer.

PP2A activity assay. Protein phosphatase 2A (PP2A) activity was measured in fresh cells as already described by us (2) using R&D Systems PP2A DuoSet IC activity assay kit according to the manufacturer's description. An immobilized capture antibody specific for the catalytic subunit of PP2A binds both active and inactive PP2A. After washing away unbound material, a synthetic phosphopeptide substrate is added that is dephosphorylated by active PP2A to generate free phosphate, which is detected by a sensitive dye-binding assay using malachite green and molybdic acid.

NF-κB p65 activation. Nuclear extraction was performed on cells using a nuclear extraction kit (Active Motif, Rixensart, Belgium) (2). Five micrograms of protein extracts were tested for the NF-κB activation by using the NF-κB p65 TransAM transcription factor assay kit (Active Motif), an ELISA-based transcription factor detection assay, according to the manufacturer's instructions.

PP2Ac siRNA. Combinations of three short inhibiting RNAs (siRNAs) targeting different positions within the β-isoform of human PP2Ac mRNA (PP2Ac-siRNA) were used (Qiagen), and a nonsilencing siRNA (non-PP2A) was included as control (17). Transfection of cells was carried out by electroporation using Lipofectamine 2000 (Invitrogen). Analyses were performed 14 h after transfection.

Measurement of airway hyperreactivity. Airway hyperreactivity was measured in conscious, unrestrained mice in a preconditioned whole body plethysmograph (Buxco Electronics, Troy, NY). BALB/c mice (*n* = 8 per group) were exposed to high CO₂ concentrations (0, 5, 10, or 15% with a constant O₂ concentration of 21%) injected directly in the plethysmograph chambers for 60 min. Respiratory parameters were recorded, and enhanced pause (Penh), which reflects pulmonary resistance (11, 22), was calculated using iox2 software (emka Technologies, Paris, France).

Mouse hypercapnia 1-h-long exposure. Thirty-two male BALB/c mice 6–7 wk old (8 mice per group) were administered nonrestrictively with high concentrations of carbon dioxide in a large plethysmography chamber (PLT-UN2-GT; emka Technologies) for 60 min at room temperature. The partial CO₂ and O₂ pressures in the chamber were measured every 2 min and every 1 min, respectively, using specific microelectrodes (Lazar Research Laboratories). In all cases, the O₂ concentration was maintained at 149 mmHg by the injection of a pure dry O₂ gas capsule (Carboxique). The CO₂ concentration was maintained by the injection of a pure dry CO₂ gas capsule (Carbox-

ique) at 35.5 mmHg (5%), 71 mmHg (10%), and 106.5 mmHg (15%). The partial H₂O pressure was estimated at ~50 mmHg.

Lung cell purification. Mice were killed 4 h after exposure to CO₂ (intraperitoneal injection of 800 μl of a 5% aqueous urethane solution). Lungs were deblooded by severing of the inferior vena cava, washed in situ with PBS, and removed. Left lungs were frozen for RNase protection assay, and right lungs were finely chopped and homogenized in a medium containing 30 mg/ml DNase I (Sigma) and 150 U/l type 4 collagenase (Worthington, Lakewood, NJ) in a Hei-dolph homogenizer (RZR 2102). Digestion took place for 1 h at 37°C. Following digestion, the red blood cells were lysed. The homogenate was passed over a cell strainer, and the single cell suspension was washed in HBSS. Cells were resuspended in culture medium and counted.

Western blot analysis of mucin 5AC in mouse lungs. Total lung cell suspensions were prepared 4 h after treatment, and total protein fractions were extracted and quantified after homogenization at 4°C in RIPA buffer containing 0.1 ml/ml PMSF (Sigma), 100 μM benzamide (Sigma), and 100 mM Na₂PO₄ (Prolabo) as protease inhibitors. Total proteins (50 μg) were separated on a 11% SDS-PAGE, and protein bands were transferred onto PVDF membranes (Millipore, Bedford, MA) and probed with goat polyclonal IgG Mucin 5AC (K-20) (Santa Cruz Biotechnology, Santa Cruz, CA) and β-actin mouse monoclonal antibody (AC-15; Abcam, Cambridge, United Kingdom). Immunoreactivity was revealed with horseradish peroxidase-conjugated donkey anti-goat IgG (Santa Cruz Biotechnology) and goat anti-mouse IgG (Santa Cruz Biotechnology) secondary antibodies. The immune complex was revealed by an enhanced chemiluminescence detection system (Amersham).

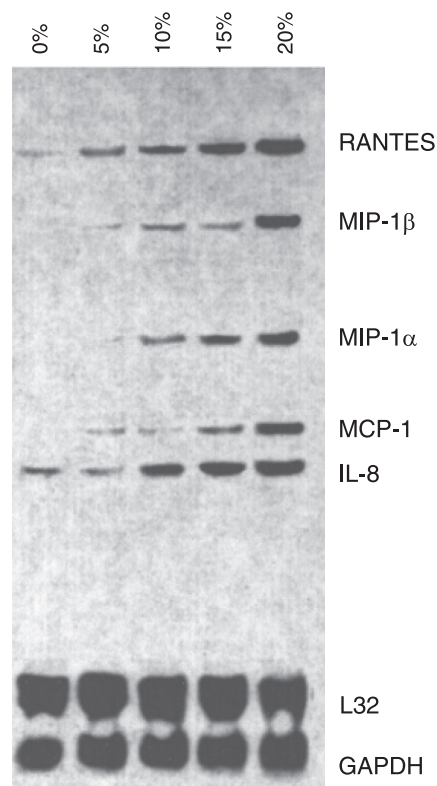


Fig. 1. Proinflammatory cytokines transcription following exposure of HT-29 to CO₂. Cytokine transcription was analyzed by RNase protection assay performed on RNA from human HT-29 cells exposed for 48 h to increased CO₂ levels with a constant O₂ concentration of 21%. Carbon dioxide increases the level of transcription of regulated upon activation, normal T cell expressed, and, presumably, secreted (RANTES), macrophage inflammatory protein-1β (MIP-1β), MIP-1α, monocyte chemoattractant protein-1 (MCP-1), and IL-8. L32 and GAPDH transcription are not altered.

Cytokine ELISpot assay. For enzyme-linked ImmunoSpot (ELISpot) assay of IL-6 and regulated upon activation, normal T cell expressed, and, presumably, secreted (RANTES), we used anti-mouse IL-6 or RANTES ELISpot kit from R&D Systems. Cells were briefly seeded onto PVDF-backed microplates (MultiScreen; Millipore) coated with cytokine-specific antibodies at a concentration of 2×10^5 cells per well. Cells were cultivated in duplicate for 20 h. Unbound cells were washed away, and a biotinylated antibody specific for the given cytokine was added. Spots (corresponding to

cytokine-secreting cells) were developed as described, and the number of spot-forming cells (SFC) was determined using a dissecting microscope (1).

Statistical analysis. The nonparametric distribution-free Kruskal-Wallis test was used to compare three or more independent groups of sampled data. When significant differences were found, Tukey multiple comparisons tests were carried out to identify which groups are different. Dose dependence of cytokine production was tested by means of ANOVA and regression analysis. All statistical analyses

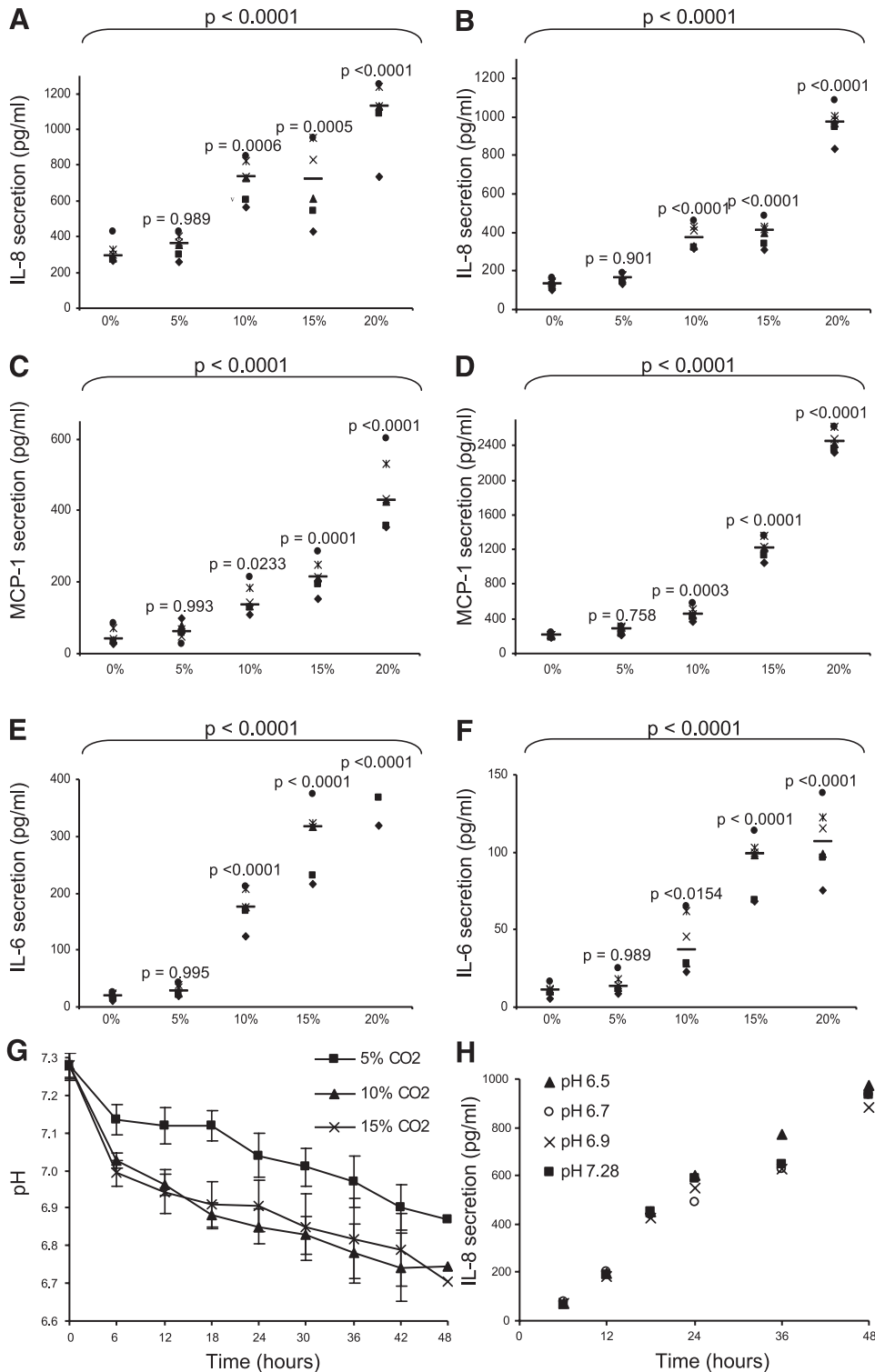


Fig. 2. Increased cytokine secretion following exposure to CO₂. A–F: cytokine secretion (ELISA, in picograms per milliliter) of human HT-29 (A, C, and E) and A549 cells (B, D, and F) exposed to increasing CO₂ concentrations for 48 h with a constant O₂ concentration of 21%. A and B, IL-8 secretion [HT-29: control (194.61–432.31); 15% (284.29–1,158.18)]; C and D, MCP-1 secretion [HT-29: control (3.82–95.63); 15% (127.44–308.43)]; E and F, IL-6 secretion [HT-29: control (9.28–30.21); 15% (177.48–415.10)]. For each group, the horizontal bar is the median. *Top* values represent the global *P* values (Kruskal-Wallis test). The *P* value given by the Tukey test above a strip chart indicates the result of the comparison of this group vs. control. Confidence interval (CI) at 96.9% are given in parentheses ($n = 6$). G: evolution of the pH of HT-29 cells medium during 48-h culture in the presence of 5, 10, or 15% CO₂ ($n = 6$). H: IL-8 secretion of HT-29 cells exposed to acidic culture medium (pH 6.5, 6.7, and 6.9 vs. control 7.28) for 48 h ($n = 5$). No significant variation was induced by acidosis.

were performed using R software (27). Values were considered statistically significant when P was <0.05 .

RESULTS

In a first step, we used colonic HT-29 and pulmonary A549 cancer cell lines to assess the overall response of epithelial cells to carbon dioxide. Exposure of HT-29 cells to carbon dioxide with a constant O₂ concentration of 21% results in the increase of the transcription of multiple chemokine genes responsible for the immune response such as the RANTES or CCL5 chemokine gene, which encodes for an 8-kDa protein, chemotactic for T and natural killer (NK) cells or MIP-1 α and MIP-1 β (Fig. 1). Likewise, there is an increased transcription of MCP-1. Proinflammatory cytokines, such as IL-8, are also increased. On the contrary, the transcription of the ribosomal L32 and GAPDH is not altered by increasing CO₂ concentrations.

These data are confirmed by the ELISA analysis of HT-29 and A549 cells (Fig. 2). The cell lines were exposed for 48 h to various concentrations of carbon dioxide. Both cell lines respond similarly to carbon dioxide. Exposure to 5% CO₂ does not appear to be toxic, as there is no difference in cytokines secretion ($P = 0.993$ for MCP-1 secretion by HT-29 cells between 0 and 5% CO₂). Above 10% carbon dioxide, there is an induction of the secretion of MCP-1 ($P < 0.0001$ between 0 and 15% CO₂ in HT-29 cells and in A549 cells), IL-6, and IL-8 ($P < 0.0001$ for difference between 0 and 15% CO₂ in A549 cells). Statistical analyses revealed a highly significant dose dependence between carbon dioxide levels and proinflammatory cytokines produced (for instance, MCP-1: $P < 0.0001$).

Because its variation could be an important element in the induction of the inflammatory response, pH was measured in culture media: for instance, in HT-29 wells (Fig. 2G), mean pH

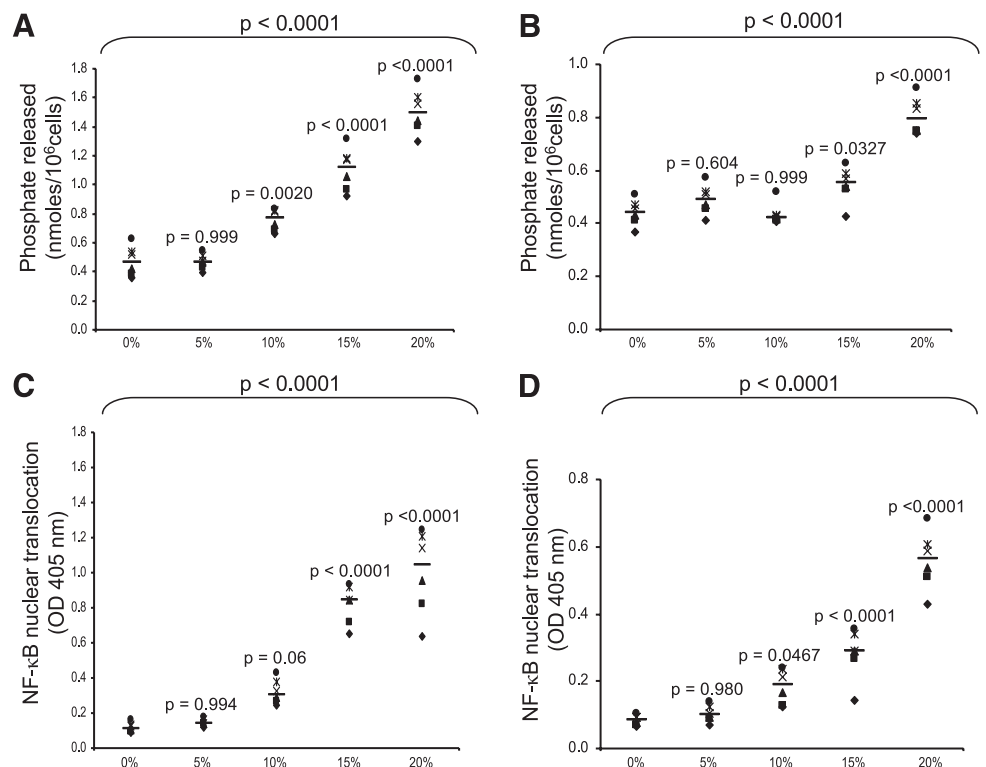
value ($n = 6$) was 7.28 in the initial culture media and 6.87 after 48-h culture with 5% CO₂, whereas it was 6.71 after 48 h culture with 15% CO₂. Thus pH changes might explain part of the observed inflammatory response induced by hypercapnia. However, in an independent experiment, we exposed HT-29 cells to almost constant acidic pH (6.5, 6.7, and 6.9) compared with 7.28 control condition, and we did not find any significant change in cytokines secretion (IL-6, data not shown; IL-8, Fig. 2H) until 48 h of culture. Thus acidity is not sufficient to induce the proinflammatory response of these cells. This highlights the fact that carbon dioxide toxicity has a mechanism of action independent of pH.

To decipher the mechanism of action of carbon dioxide, we measured the activity of PP2A and of NF- κ B. In previous papers (2, 29), we reported that PP2A controls the translocation from the cytoplasm to the nucleus of p65 NF- κ B.

Increased concentration of carbon dioxide stimulates the activity of PP2A such as the release of phosphate (Fig. 3, A and B; $P < 0.0001$ in HT-29 cells and $P < 0.05$ in A549 cells for difference between 0 and 15% CO₂). According to our previous work, a translocation from the cytoplasm to the nucleus of p65 NF- κ B takes place (Fig. 3, C and D). A549 and HT-29 cancer cell lines respond similarly to carbon dioxide ($P < 0.0001$ for difference between 0 and 15% CO₂ in HT-29 cells or in A549 cells).

To confirm the key role of PP2A in CO₂-induced inflammation, we transfected both A549 and HT-29 cancer cells with silencing RNA. The cells were either treated with nonspecific siRNA or with siRNAs targeted toward the catalytic subunit of PP2A (17). Figure 4 shows that transfection with siRNAs targeted toward the catalytic subunit of PP2A significantly diminishes the effect of 15% carbon dioxide (at least 50%). After transfection, treatment with carbon dioxide fails to in-

Fig. 3. Protein phosphatase 2A (PP2A) and NF- κ B activation in response to in vitro carbon dioxide exposure. A and B: measurement of the amount of phosphate released by PP2A (nanomoles per 10⁶ cells) in HT-29 (A) and A549 (B) cells after exposure to CO₂ with a constant O₂ concentration of 21% for 48 h [HT-29: control (0.272–0.674); 15% (0.809–1.398)]. C and D: measurement of p65 NF- κ B nuclear translocation [optical density (OD) 405 nm] in HT-29 (C) and A549 (D) cells after exposure to CO₂ with a constant O₂ concentration of 21% for 48 h [HT-29: control (0.062–0.176); 15% (0.602–1.038)]. For each group, the horizontal bar is the median. Top values represent the global P values (Kruskal-Wallis test). The P value given by the Tukey test above a strip chart indicates the result of the comparison of this group vs. control. CI at 96.9% are given in parentheses ($n = 6$).



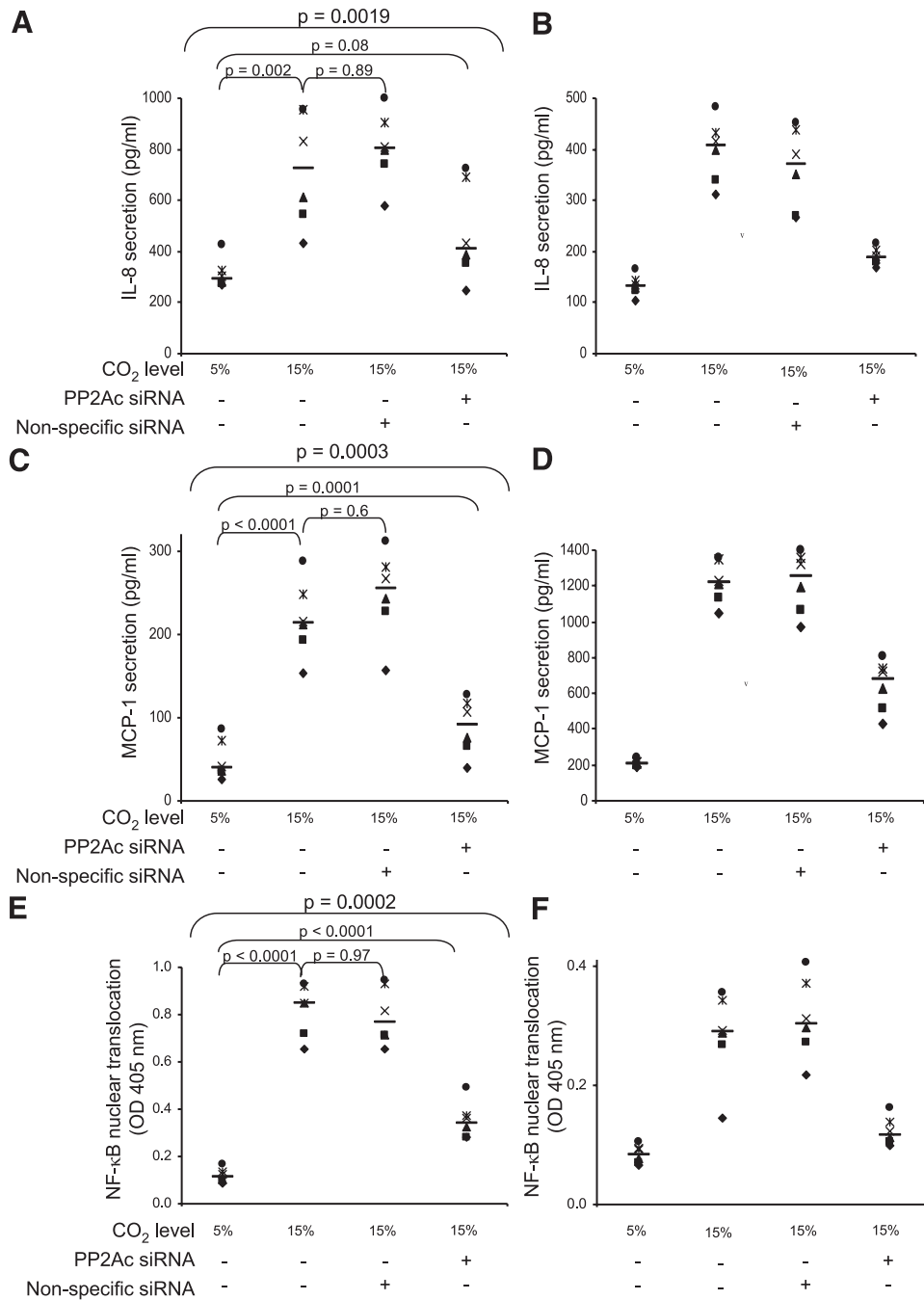


Fig. 4. Effect of PP2Ac short inhibiting RNAs (siRNAs) on the inflammatory reaction caused by CO₂ exposure in HT-29 and A549 cells. Human HT-29 (A, C, and E) and A549 (B, D, and F) cells were transfected with PP2Ac specific and nonspecific siRNAs and then incubated with increasing CO₂ levels (with a constant O₂ concentration of 21%) for 14 h (*n* = 6). IL-8 [A and B; HT-29: 15% CO₂ (431.28–954.63), 15% CO₂ + PP2Ac siRNA (246.52–722.14)] and MCP-1 [C and D; HT-29: 15% CO₂ (153.17–287.5), 15% CO₂ + PP2Ac siRNA (39.18–128.11)] proinflammatory cytokine production (ELISA, in picograms per milliliter) is reduced in the presence of PP2Ac siRNAs. NF-κB nuclear translocation [E and F; OD 405 nm; HT-29: 15% CO₂ (0.652–0.944), 15% CO₂ + PP2Ac siRNA (0.28–0.491)] is specifically inhibited by PP2Ac siRNAs. For each group, the horizontal bar is the median. *Top* values represent the global *P* values (Kruskal-Wallis test). The *P* value given by the Tukey test above a strip chart indicates the result of the comparison of this group vs. control. CI at 96.9% are given in parentheses (*n* = 6).

crease the level of IL-8 (Fig. 4, A and B; *P* < 0.001 for difference between 15% CO₂ and 15% CO₂ + PP2Ac siRNA by A549 cells) and MCP-1 (Fig. 4, C and D; *P* = 0.0001 for difference between 15% CO₂ and 15% CO₂ + PP2Ac siRNA by HT-29 cells). The nuclear translocation of NF-κB is abolished (Fig. 4, E and F; *P* < 0.0001 for difference between 15% CO₂ and 15% CO₂ + PP2Ac siRNA by HT-29 cells or A549 cells). As expected, nonspecific siRNA has no effect on the secretion of IL-8, MCP-1, or on the nuclear translocation of NF-κB. We completed the results obtained on human cancer cell lines by in vivo experiments.

Normal total lung cells (mixture of primary lung cells) were retrieved from mice exposed to carbon dioxide for 1 h

(with a constant O₂ concentration of 21%). These cells were then cultured for 20 h to perform RNase protection assay, ELISA, and ELISpot proinflammatory cytokine measurements. Like human cancer cells, these murine normal cells respond to carbon dioxide (Fig. 5). There is an increase of the RNA transcription of proinflammatory chemokines, such as RANTES, MIP-1α, MIP-1β, and MCP-1 (Fig. 5A). Likewise, there was an increased transcription of the genes encoding for TCA-3 (T-cell activation gene), a proinflammatory protein produced by T lymphocytes, eotaxin, a chemokine implicated in allergy and inflammation, and IP-10 (interferon-γ-induced protein 10 or CXCL10), a chemokine implicated in inflammation.

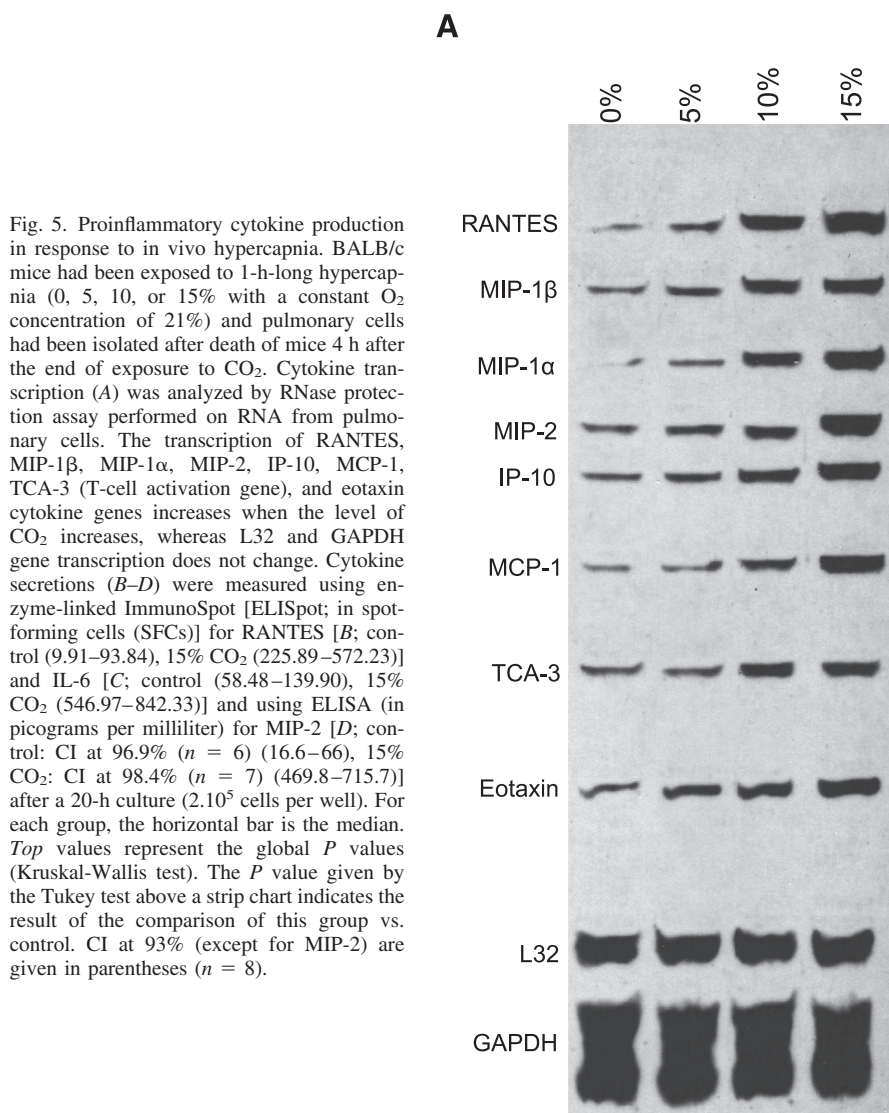


Fig. 5. Proinflammatory cytokine production in response to in vivo hypercapnia. BALB/c mice had been exposed to 1-h-long hypercapnia (0, 5, 10, or 15% with a constant O₂ concentration of 21%) and pulmonary cells had been isolated after death of mice 4 h after the end of exposure to CO₂. Cytokine transcription (A) was analyzed by RNase protection assay performed on RNA from pulmonary cells. The transcription of RANTES, MIP-1 β , MIP-1 α , MIP-2, IP-10, MCP-1, TCA-3 (T-cell activation gene), and eotaxin cytokine genes increases when the level of CO₂ increases, whereas L32 and GAPDH gene transcription does not change. Cytokine secretions (B–D) were measured using enzyme-linked ImmunoSpot [ELISpot; in spot-forming cells (SFCs)] for RANTES [B; control (9.91–93.84), 15% CO₂ (225.89–572.23)] and IL-6 [C; control (58.48–139.90), 15% CO₂ (546.97–842.33)] and using ELISA (in picograms per milliliter) for MIP-2 [D; control: CI at 96.9% ($n = 6$) (16.6–66), 15% CO₂: CI at 98.4% ($n = 7$) (469.8–715.7)] after a 20-h culture (2.10⁵ cells per well). For each group, the horizontal bar is the median. Top values represent the global P values (Kruskal-Wallis test). The P value given by the Tukey test above a strip chart indicates the result of the comparison of this group vs. control. CI at 93% (except for MIP-2) are given in parentheses ($n = 8$).

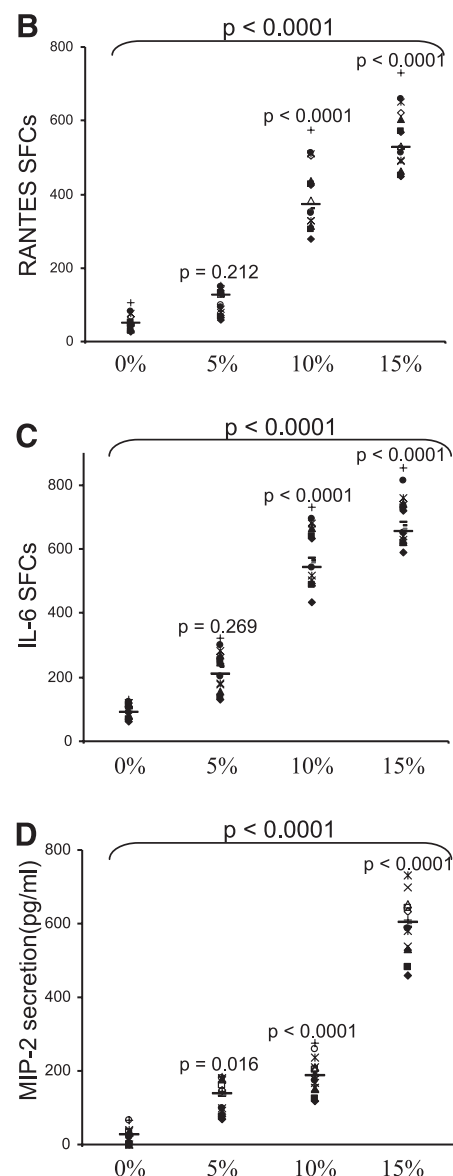


Figure 5, B–D, shows that there is an increase in cytokine secretion by pulmonary cells isolated from mice exposed to 1-h-long hypercapnia. Cytokines were measured using ELISpot for RANTES (Fig. 5B; $P < 0.0001$ for difference between 0 and 15% CO₂) and IL-6 (Fig. 5C; $P < 0.0001$ for difference between 0 and 15% CO₂) and using ELISA for MIP-2 (Fig. 5D; $P < 0.0001$ for difference between 0 and 15% CO₂) after a 20-h culture. As shown in vitro, PP2A (Fig. 6A) and NF- κ B (Fig. 6B) activations are induced in lung cells exposed to carbon dioxide. Thus it is very likely that both in vivo and in vitro cytokine secretion following exposure to carbon dioxide is mediated by PP2A and NF- κ B translocation.

Exposure of mice to carbon dioxide causes an inflammatory syndrome. We measured the impact of carbon dioxide exposure on mucin 5AC expression, which is a major pulmonary mucus glycoprotein overexpressed during inflammation [notably chronic obstructive pulmonary disease (COPD) and asthma] and bacterial infections (36). Increased concentration of carbon dioxide results in enhanced production of mucin

5AC protein (Fig. 7A). The effect of 5% carbon dioxide appears limited. The effect of higher doses is more striking.

Penh is a well-accepted marker of airway reactivity (11). Mice were exposed while in a barometric plethysmography chamber for 60 min to various concentrations of carbon dioxide (normal air and 5, 10, and 15% with a constant O₂ concentration of 21%, $n = 8$). Penh, which reflects airway obstruction, was measured every minute during the experiment, and, for each time point and group, the average values are presented (Fig. 7B). Inhalation of CO₂, and especially of 15% CO₂, increases the reactivity of the airway as shown by Penh increase in hypercapnic conditions. During this acute experiment, the airway hyperreactivity is only slightly dependent on the duration of exposure.

These studies demonstrate the inflammatory effect of carbon dioxide. Nevertheless, there appears to be a threshold. Our work suggests the innocuity of 5% carbon dioxide, a concentration that is similar to the carbon dioxide concentration in the alveolar sac (18).

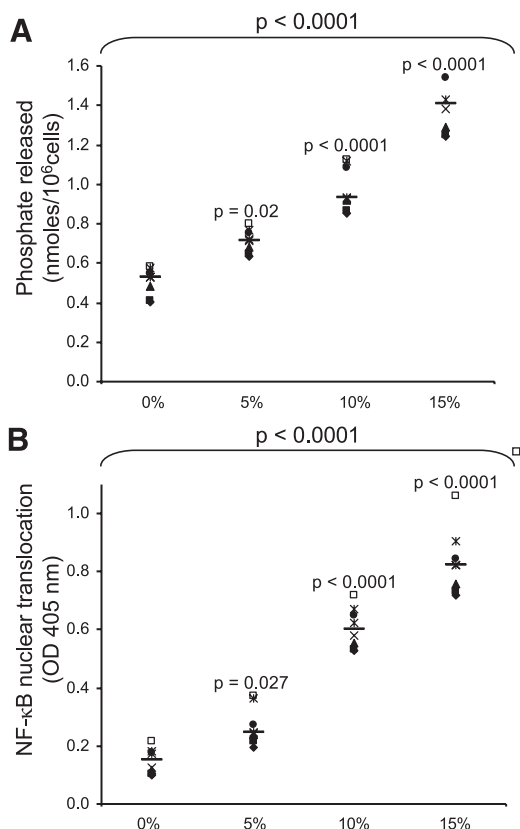


Fig. 6. PP2A and NF- κ B activation in response to in vivo hypercapnia. BALB/c mice had been exposed to 1-h-long hypercapnia (0, 5, 10, or 15% with a constant O₂ concentration of 21%) and pulmonary cells had been isolated after death of mice 4 h after the end of exposure to CO₂. The amount of phosphate released by PP2A (A) and the p65 NF- κ B nuclear translocation (B) were measured [PP2A: control (0.37–0.64), 15% CO₂ (1.04–1.87); NF- κ B: control (0.06–0.23), 15% CO₂ (0.61–1.05)]. For each group, the horizontal bar is the median. Top values represent the global *P* values (Kruskal-Wallis test). The *P* value given by the Tukey test above a strip chart indicates the result of the comparison of this group vs. control. CI at 93% are given in parentheses (*n* = 8).

DISCUSSION

In a first attempt to decipher the potential inflammatory role of carbon dioxide, we show the deleterious effect of short-term exposure to CO₂ with a constant O₂ concentration of 21%. In vitro exposure to 5% CO₂ has only a limited effect if any. This may be due in part to the fact that cells are usually grown in 5% CO₂. Above this threshold, there clearly is a dose-dependent response in the secretion of multiple proinflammatory cytokines. This secretion is plausibly mediated by the nuclear translocation of p65 NF- κ B, itself a consequence of PP2A activation. siRNAs targeted toward PP2Ac reverse the effect of carbon dioxide.

PP2A comprises a family of serine-threonine phosphatases implicated in regulation of many signaling pathways and, in particular, inflammation. PP2A holoenzyme is composed of an association of three subunits: 1) regulatory; 2) structural; and 3) catalytic. One of the functions of the methylated and active PP2Ac is the activation of NF- κ B pathway (19). This pathway has been deciphered in other instances, most notably hyperosmotic stress (2) or during immune response (29). In fact, we previously demonstrated that hyperosmotic stress response of

HT-29 cells is mostly dependant on PP2A activation (methylation). This stimulates IKK γ complex and induces I κ B α degradation leading to NF- κ B nuclear translocation and proinflammatory mediators secretion. In the case of carbon dioxide, we can assert that the inflammatory response is mediated at least in part by PP2A and NF- κ B pathways.

Our data are consistent with the literature. Niemoeller and Schaefer (25) exposed guinea pigs and rats to different CO₂ concentrations (for 2–42 days at 1.5, 3, and 15% CO₂ in 21% O₂). They noticed extensive lung inflammation with loss of surfactant, hyaline membrane formation (present at 3% CO₂ for 4 days and in all animals at 15% CO₂ for 1–2 days), and atelectasis (from 1.5% CO₂). Hyaline membrane formation was associated with respiratory distress syndrome (25).

In a follow-up study (28), guinea pigs were exposed to up to 15% CO₂. The authors identified four phases of pulmonary changes caused by 15% carbon dioxide. The initial phase (6 h) was marked by respiratory acidosis accompanied by pulmonary inflammation (edema, congestion, atelectasis, and hemorrhage) and changes in the lamellar bodies (intracellular stores of surfactant) of the granular (type II) pneumocytes. The second phase (6–24 h) was associated with hyaline membrane formation. During the third phase (*days* 2–7), the surface tension returned to normal, the pulmonary edema diminished, and hyaline membranes disappeared. The final phase was one of recovery, although the CO₂ concentration remained high.

The role of CO₂ in inflammation has long been controversial. Very high concentrations (>90%) have been reported to decrease the risk of peritonitis after coelioscopy (12). This type of insufflation causes transient and local acidification that inhibits LPS-stimulated release of proinflammatory cytokines (IL-1 and TNF) by macrophages (37). However, in isolated alveolar type II epithelial cells, cell injury, mediated by nitric oxide activity, was enhanced in cells exposed to high concentrations of CO₂ (20).

Smoking is one of the leading causes of death worldwide. For most authors, the toxicity is mostly linked to tar, a complex mixture of thousands of chemicals, such as polycyclic aromatic hydrocarbons and nitrosamines (14). However, the exact role of each cigarette smoke component in lung carcinogenesis is not really defined. In addition to cytotoxic compounds found in the particulate phase, the vapor phase of mainstream cigarette smoke contains a number of cytotoxic constituents capable of damaging cells and inducing pulmonary inflammation (30). A large body of evidence suggests that smoking-induced pulmonary inflammation may play an important role in increasing lung cancer risk in smokers (8, 21, 31, 33).

The combustion of tobacco like any carbon-rich compound releases CO₂ (12.5% by weight in whole mainstream smoke). Our data suggest that concentrations of CO₂ such as the one released during combustion cause inflammation of the respiratory tract.

The toxicity of tobacco smoke is not limited to the acute inflammation of the respiratory tract. It has other side effects, i.e., cardiovascular and central (3). Long-term side effects include reproductive problems, teratogenicity, and most importantly carcinogenesis. The purpose of the following paragraphs is to suggest that the toxicity of smoke can be mimicked by CO₂ inhalation.

One of the first effects of CO₂ inhalation is an increase in cardiac activity. As of 5% CO₂, the first signs of cardiovascular

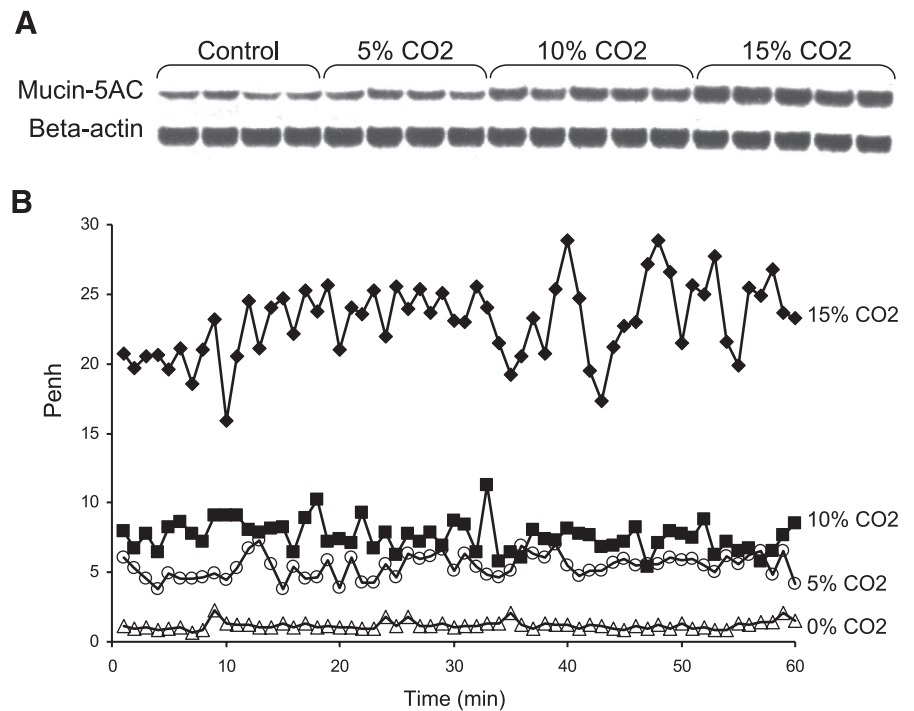


Fig. 7. Lung inflammation in response to in vivo hypercapnia. BALB/c mice had been exposed to 1-h-long hypercapnia (0, 5, 10, or 15% with a constant O₂ concentration of 21%). *A*: induction of mucin 5AC production by hypercapnia-exposed pulmonary cells revealed by Western blot analysis. For each condition, 4 or 5 samples from different animals were loaded. β -Actin is used as a control. *B*: induction of mouse airway hyperreactivity by hypercapnia was measured in BALB/c mice ($n = 8$ per group) exposed to increasing CO₂ concentrations (0, 5, 10, and 15% with a constant O₂ concentration of 21%) for 60 min. Enhanced pause (Penh), which reflects airway obstruction, was measured by barometric plethysmography every minute during the experiment; average values are presented.

and vasomotor impacts (cardiac frequency and arterial pressure, peripheral vasodilatation) appear in human beings. The same symptoms are observed in dogs and monkeys, at concentrations up to 10% (32). Similarly, respiratory rate is increased twofold until 10% CO₂ is reached, whereas above 10% it is reduced. In dogs with left ventricular failure (embolization of the left coronary artery), hypercapnia aggravated the heart failure (38).

In rats (34), carbon dioxide causes degenerative modifications of the testis depending on the concentration (2.5, 5, and 10% CO₂ + 20% O₂ up to 100% with nitrogen) and on the duration of exposure (1–8 h). Major histological effects included tubular disturbances such as sloughing as well as loss of luminal definition (5% for 4 h) and degenerative changes such as streaking and vacuolization (10% for 4 h). A concentration of 15% CO₂ has a marked effect on spermatogenesis of guinea pigs and rats (30). The first changes in spermatogenesis are noted after 48 h of exposure to 15% CO₂ when a notable reduction in the number of mature spermatocytes becomes apparent and is associated with an increase in their precursors. After 3–7 days, multinucleated giant cells are seen.

Exposure of rats to 6% carbon dioxide (single 24-h period between *days 5* and *21* of pregnancy) causes cardiac (24 vs. 7% in controls) and skeletal malformations (11 vs. 0.6% in controls) in the newborn pups (13). In rabbits exposed to 10–13% carbon dioxide, the newborn kittens had vertebral malformations (10). Ten percent CO₂ and consecutive acidosis of neonatal rats promote the retinopathy of prematurity (15, 16). Nagai et al. (24) showed that rabbit fetuses (exposed from *days 21* to *28* of gestation to 8% CO₂ for 8 h each day) weighed less and presented numerous characteristics of increased tissue and cellular maturation of the lung.

Currently, there is no proof that exposure to carbon dioxide is linked to cancer. Nevertheless, there are data in the literature suggesting that exposure may have long-term deleterious effects.

For instance, concentrations of CO₂ above 12% applied to in vitro cultures induce many abnormal chromatin figures supporting the hypothesis of a role of high CO₂ concentrations in carcinogenesis via the disruption of cell division processes (23).

Our data confirm the inflammatory effect of CO₂ at levels higher than the normal concentration in ambient air but similar to the inhaled smoke. Similarly to hyperosmotic shock (2, 29), the toxicity of carbon dioxide is partly mediated by the activation of PP2A, which results in the translocation of NF- κ B. The mechanism of action of CO₂ might also involve the inhibition of the Krebs cycle and glycolysis for stoichiometric reasons.

Smokers are prone to multiple diseases and have a shortened life expectancy. Smokers age faster than the nonexposed population. The link between inflammation and ageing has been well established (9). Carbon dioxide may also play a role in premature ageing. In the Western world, the prevalence of the metabolic syndrome is increasing exponentially. Chronic subacute inflammation characterizes the syndrome, suggesting that inflammation might be a common denominator that links obesity to its pathological sequelae. Increased exogenous or endogenous CO₂ deoxygenates hemoglobin, thereby increasing the fraction of hemoglobin reacting with nitrite to form methemoglobin together with release of superoxide and nitric oxide. These may form peroxynitrite, which may cause inflammation and premature ageing (39).

The role of CO₂ in ageing has not been explored. It is our hypothesis that chronic intermittent exposure to carbon dioxide will be a powerful tool for the investigation of the intertwined links between inflammation, ageing, and cancer.

ACKNOWLEDGMENTS

We acknowledge the help of Georges Grévillet, Xavier Wertz, and Jean-Marc Steyaert.

GRANTS

This work was funded by Biorébus.

REFERENCES

1. Abolhassani M, Lagranderie M, Chavarot P, Balazuc AM, Marchal G. *Mycobacterium bovis* BCG induces similar immune responses and protection by rectal and parenteral immunization routes. *Infect Immun* 68: 5657–5662, 2000.
2. Abolhassani M, Wertz X, Pooya M, Chaumet-Riffaud P, Guais A, Schwartz L. Hyperosmolarity causes inflammation through the methylation of protein phosphatase 2A. *Inflamm Res* 57: 419–429, 2008.
3. Ambrose JA, Barua RS. The pathophysiology of cigarette smoking and cardiovascular disease: an update. *J Am Coll Cardiol* 43: 1731–1737, 2004.
4. Beychok MR. *Fundamentals of Stack Gas Dispersion* (4th ed.), edited by Beychok MR. Newport Beach, CA: M R Beychok, 2005.
5. Castro P, Legora-Machado A, Cardilo-Reis L, Valença S, Porto LC, Walker C, Zuany-Amorim C, Koatz VL. Inhibition of interleukin-1 β reduces mouse lung inflammation induced by exposure to cigarette smoke. *Eur J Pharmacol* 498: 279–286, 2004.
6. Dhami R, Gilks B, Xie C, Zay K, Wright JL, Churg A. Acute cigarette smoke-induced connective tissue breakdown is mediated by neutrophils and prevented by α 1-antitrypsin. *Am J Respir Cell Mol Biol* 22: 244–252, 2000.
7. Dube MF, Green CR. Methods of collection of smoke for analytical purposes. *Recent Adv Tob Sci* 8: 42–102, 1982.
8. Engels EA. Inflammation in the development of lung cancer: epidemiological evidence. *Expert Rev Anticancer Ther* 4: 605–615, 2008.
9. Finch CE. *The Biology of Human Longevity*. Burlington, MA: Academic Press, 2007.
10. Grote W. Disturbances of embryonic development at elevated CO₂ and O₂ partial pressure at reduced atmospheric pressure. *Z Morphol Anthropol* 56: 165–194, 1965.
11. Hamelmann E, Schwarze J, Takeda K, Oshiba A, Larsen GL, Irvin CG, Gelfand EW. Noninvasive measurement of airway responsiveness in allergic mice using barometric plethysmography. *Am J Respir Crit Care Med* 156: 766–775, 1997.
12. Hanly EJ, Aurora AA, Shih SP, Fuentes JM, Marohn MR, De Maio A, Talamini MA. Peritoneal acidosis mediates immunoprotection in laparoscopic surgery. *Surgery* 142: 357–364, 2007.
13. Haring OM. Cardiac malformation in rats induced by exposure of the mother to carbon dioxide during pregnancy. *Circ Res* 8: 1218–1227, 1960.
14. Hecht SS. Cigarette smoking: cancer risks, carcinogens, and mechanisms. *Langenbecks Arch Surg* 391: 603–613, 2006.
15. Holmes JM, Duffner LA, Kappil JC. The effect of raised inspired carbon dioxide on developing rat retinal vasculature exposed to elevated oxygen. *Curr Eye Res* 13: 779–782, 1994.
16. Holmes JM, Zhang S, Leske DA, Lanier WL. Carbon dioxide-induced retinopathy in the neonatal rat. *Curr Eye Res* 17: 608–616, 1998.
17. Katsiari CG, Kyttaris VC, Juang YT, Tsokos GC. Protein phosphatase 2A is a negative regulator of IL-2 production in patients with systemic lupus erythematosus. *J Clin Invest* 115: 3193–3204, 2005.
18. Koulouris NG, Latsi P, Dimitroulis J, Jordanoglou B, Gaga M, Jordanoglou J. Noninvasive measurement of mean alveolar carbon dioxide tension and Bohr's dead space during tidal breathing. *Eur Respir J* 17: 1167–1174, 2001.
19. Kray AE, Carter RS, Pennington KN, Gomez RJ, Sanders LE, Llanes JM, Khan WN, Ballard DW, Wadzinski BE. Positive regulation of IkappaB kinase signaling by protein serine/threonine phosphatase 2A. *J Biol Chem* 280: 35974–35982, 2005.
20. Lang JD Jr, Chumley P, Eiserich JP, Estevez A, Bamberg T, Adhami A, Crow J, Freeman BA. Hypercapnia induces injury to alveolar epithelial cells via a nitric oxide-dependent pathway. *Am J Physiol Lung Cell Mol Physiol* 279: L994–L1002, 2000.
21. Littman AJ, Thornquist MD, White E, Jackson LA, Goodman GE, Vaughan TL. Prior lung disease and risk of lung cancer in a large prospective study. *Cancer Causes Control* 15: 819–827, 2004.
22. Lundblad LK, Irvin CG, Adler A, Bates JH. A reevaluation of the validity of unrestrained plethysmography in mice. *J Appl Physiol* 93: 1198–1207, 2002.
23. Mottram J. On the division of cells under varying tensions of carbon dioxide. *Br J Exp Pathol* 9: 240–244, 1928.
24. Nagai A, Thurlbeck WM, Deboeck C, Ioffe S, Chernick V. The effect of maternal CO₂ breathing on lung development of fetuses in the rabbit. Morphologic and morphometric studies. *Am Rev Respir Dis* 135: 130–136, 1987.
25. Niemoeller H, Schaefer KE. Development of hyaline membrane and atelectases in experimental chronic respiratory acidosis. *Proc Soc Exp Biol Med* 110: 804–808, 1962.
26. Norman V. An overview of the vapor phase, semivolatile and nonvolatile components of cigarette smoke. *Recent Adv Tob Sci* 3: 28–58, 1977.
27. R Development Core Team. *R: A Language and Environment for Statistical Computing* (Online). R Foundation for Statistical Computing, Vienna, Austria, 2006. <http://www.r-project.org>.
28. Schaefer KE, Avery ME, Bensch K. Time course of changes in surface tension and morphology of alveolar epithelial cells in CO₂-induced hyaline membrane disease. *J Clin Invest* 43: 2080–2093, 1964.
29. Schwartz L, Abolhassani M, Pooya M, Steyaert JM, Wertz X, Israël M, Guais A, Chaumet-Riffaud P. Hyperosmotic stress contributes to mouse colonic inflammation through the methylation of protein phosphatase 2A. *Am J Physiol Gastrointest Liver Physiol* 295: G934–G941, 2008.
30. Smith CJ, Perfetti TA, Garg R, Hansch C. IARC carcinogens reported in cigarette mainstream smoke and their calculated log P values. *Food Chem Toxicol* 41: 807–817, 2003.
31. Smith CJ, Perfetti TA, King JA. Perspectives on pulmonary inflammation and lung cancer risk in cigarette smokers. *Inhal Toxicol* 18: 667–677, 2006.
32. Stinson JM, Mattsson JL. Tolerance of rhesus monkeys to graded increase in environmental CO₂: serial changes in heart rate and cardiac rhythm. *Aerospace Med* 42: 78–80, 1970.
33. Trichopoulos D, Psaltopoulou T, Orfanos P, Trichopoulou A, Boffetta P. Plasma C-reactive protein and risk of cancer: a prospective study from Greece. *Cancer Epidemiol Biomarkers Prev* 15: 381–384, 2006.
34. VanDemark NL, Schanbacher BD, Gomes WR. Alterations in testes of rats exposed to elevated atmospheric carbon dioxide. *J Reprod Fertil* 28: 457–459, 1972.
35. Van der Vaart H, Postma DS, Timens W, ten Hacken NH. Acute effects of cigarette smoke on inflammation and oxidative stress: a review. *Thorax* 59: 713–721, 2004.
36. Voynow JA, Gendler SJ, Rose MC. Regulation of mucin genes in chronic inflammatory airway diseases. *Am J Respir Cell Mol Biol* 34: 661–665, 2006.
37. West MA, Hackam DJ, Baker J, Rodriguez JL, Bellingham J, Rotstein OD. Mechanism of decreased in vitro murine macrophage cytokine release after exposure to carbon dioxide. *Ann Surg* 226: 179–190, 1997.
38. Wexels JC, Mjøs OD. Effects of carbon dioxide and pH on myocardial function in dogs with acute left ventricular failure. *Crit Care Med* 15: 1116–1120, 1987.
39. Zappulla D. Environmental stress, erythrocyte dysfunctions, inflammation, and the metabolic syndrome: adaptations to CO₂ increases? *J Cardiometaab Syndr* 3: 30–34, 2008.